JAAS

PAPER

In situ Re–Os geochronology of Re-rich Palaeogene molybdenite by LA-ICP-MS/MS†

Stijn Glorie, ®*[a] Jay M. Thompson, ® [b] Sarah E. Gilbert ® [c] and A. Kate Souders ® [b]

In situ Re–Os geochronology by LA-ICP-MS/MS was previously demonstrated by reacting Os with CH_4 or N_2O reaction gasses. However, for both reactions, a minor proportion of the Re parent isotope also reacts, potentially leading to significant isobaric interferences of ^{187}Re on ^{187}Os, especially for young samples with little radiogenic in-growth. Here we present an interlaboratory comparison and compare three reaction gas mixtures ($CH_4 + H_2 + He$, N_2O and $N_2O + He$) with the aim to robustly date Palaeogene (66–23 Ma) molybdenite from the Bingham Canyon and Henderson deposits. CH_4 mixed with H_2 gas gives the highest sensitivity, while N_2O and He gas buffer Re reaction. On balance, the analytical method involving $N_2O + He$ reaction gas is most suitable for dating Palaeogene molybdenite, resulting in age precision of 2.6% for Bingham and 5.8% for Henderson. For older, >1 Ga molybdenite, $CH_4 + H_2 + He$ may give comparatively better age precision.

Introduction

Molybdenite Re–Os geochronology is widely used in ore and hydrocarbon exploration (*e.g.* ref. 1 and 2). The conventional analytical approach involves isotope dilution followed by isotope ratio measurements with a Thermal Ionization Mass Spectrometer (TIMS), which is a laborious and time-consuming method that is conducted at highly specialized laboratories.[3,4] Recent developments in reaction gas mass-spectrometry now allow Re and Os isotopes to be rapidly measured *in situ* using laser ablation inductively coupled plasma tandem mass-spectrometry (LA-ICP-MS/MS) at high spatial resolution.[5–7] Hogmalm *et al.*[5] and Tamblyn *et al.*[6] demonstrated that Os efficiently reacts with CH_4 to form $OsCH_2^+$, inducing a +14 amu mass-shift. This reaction occurs at a much higher rate (*ca.* 120×) compared to isobaric $ReCH_2^+$ production. However, the *ca.* 1–2% Re reaction accounts for potentially significant interference on mass 201 amu ($^{187}Os^{12}C^1H_2$, referred here as $^{187+14}$Os), especially for young samples with relatively low ^{187}Os ingrowth. More recently, Simpson *et al.*[7] showed that Os reacts with N_2O to form OsO_4^+, inducing a +64 amu mass-shift for $^{187}Os^{16}O_4$ (referred here as $^{187+64}$Os). The equivalent reaction of Re can be reduced to *ca.* 0.15%, which is about an order of magnitude lower than for the CH_4 method.[6] However, while the interference correction is larger, generally, higher sensitivity (count rates) can be

achieved with the CH_4 method. The obtainable precision on the resulting Re–Os date is a balance between (1) increasing sensitivity and better counting statistics, and (2) reducing the interference correction, which also reduces count rates. Here we explore the limitations of the LA-ICP-MS/MS method on Cenozoic (<66 Ma) samples, with both the N_2O and CH_4 reaction gas methods. In addition to published reaction gas methodologies, we also explore the effects of mixing reaction gasses by adding H_2 and/or He to CH_4 or N_2O in the reaction cell. We further present the first interlaboratory comparison for the *in situ* Re–Os molybdenite dating method.

Sample descriptions

Bingham Canyon molybdenite

Molybdenite was sampled from the high-grade ore zone of the Bingham Canyon porphyry deposit in northern Utah, United States (US). This sample is a porphyritic intrusive that contains the following minerals: quartz (45%, 2 to 10 mm), altered feldspar (40%, 2 to 5 mm), biotite (~2%, 0.2 to 0.5 mm), chalcopyrite (~1%, <0.2 mm) and molybdenite (~12%, 0.5 to >5 mm). Molybdenite occurs as aggregates and veins up to 10 mm in size of several millimetre-sized individual molybdenite crystals. The selected molybdenite grains were 0.5 to 2 mm in size and separated from the whole rock sample by gentle crushing and picking of grains onto double-sided tape prior to mounting in epoxy resin. The sample was then polished using fine SiC sandpaper (1000 and 2000 grit), finished using 1 μm suspended diamond paste and cleaned with ethanol. The age of the molybdenite from this deposit is dated by conventional N-TIMS Re–Os at 37.0 ± 0.27 Ma.[8] The reported uncertainty is 2 SEM (=2 standard error of the mean).

*a*Dept. of Earth Sciences, University of Adelaide, Adelaide, SA 5005, Australia. E-mail: stijn.glorie@adelaide.edu.au

*b*U.S. Geological Survey, Denver, CO 80225, USA

*c*Adelaide Microscopy, University of Adelaide, Adelaide, SA 5005, Australia

Henderson mine/RM 8599

Molybdenite was sampled from the high-grade ore concentrate in the Henderson mine, Colorado, US. This sample was measured as individual molybdenite grains from the original porphyritic rock sample as well as the mechanically homogenized RM 8599 powder purchased from the National Institute of Standards and Technology (NIST). The molybdenite grains from the whole rock sample were 0.5 to 2 mm in size and separated from the rock matrix by gentle crushing and picking of grains onto double-sided tape prior to mounting in epoxy resin. The sample was then polished using fine SiC sandpaper (1000 and 2000 grit), finished using 1 μm suspended diamond paste and cleaned with ethanol. The RM 8599 powder was prepared by pressing ∼2 grams into a 11 mm pellet at 10 tons of pressure (30 second holding time). The conventional N-TIMS Re–Os reference age of the RM 8599 sample is 27.656 ± 0.022 Ma.[9] The individual molybdenite grains are assumed to be the same age as this molybdenite powder.

Analytical methods

The molybdenite samples were analysed at the United States Geological Survey (USGS) Denver Federal Centre (Geology, Geophysics, and Geochemistry Science Center), Colorado, US and Adelaide Microscopy, University of Adelaide, Australia, for laboratory comparison purposes.

US geological survey

At the USGS the analyses were performed in the USGS-LTRACE laboratory. A total of 6 analytical sessions are reported. Analyses from 2021 and 2022 were conducted using a Photon Machines Analyte G2 laser system with an ATL ArF excimer source operating at 193 nm wavelength and ∼5 n pulse width. Analyses from 2023 onward were conducted using a RESOlution-SE 193 nm laser ablation system also with an ATL excimer laser source. Both laser systems were coupled to an Agilent 8900x ICP-MS/MS. The laser fluence was varied between 3.5 and 6 J cm^{-2}, depending on the session, spot size was between 80 and 120 microns, and laser repetition rate was between 10 and 20 Hz. All analyses were performed in a helium atmosphere and signal smoothing of laser pulses was achieved using the 'squid' signal smoother. Nitrogen (N$_2$) was added to the Ar carrier gas before the ICP-MS to increase sensitivity.

The ICP-MS tuning was first performed in single-quad mode for maximum heavy mass sensitivity while achieving a ThO/Th rate of <0.2% and U/Th <1.1 for the S-155 ablation cell and ∼1.2 for the HelEx cell (Analyte G2). Tuning was performed using the NIST612 glass with a ∼40 micron square beam (38 micron beam for the RESOlution-SE system), 10 Hz, 3.5 J cm^{-2} and 3 microns per s line scan speed. Under these conditions, the count rate for ^{238}U was ∼1 Mcps. Once optimized in single-quad mode, the instrument was set to MS/MS mode with reaction gases CH$_4$ (6% or 0.07 ml min^{-1}), He (4.8 to 6.3 ml min^{-1}) and H$_2$ (5.0 to 5.4 ml min^{-1}). See ESI 1†[10] for further ICP-MS/MS setting details. The ^{185}Re^{12}CH$_2$/^{185}Re ratio was monitored during tuning and reaction gas flow rates and octupole settings were adjusted to minimize this ratio (∼0.3 to ∼0.4) while still maintaining

sensitivity for the ^{185}Re signal. The MASS-3 FeS pressed powder from the USGS was used for monitoring Os signal, but tuning specifically for Os was not feasible due to heterogeneities in the Os content of this material (5 to 10% variation). The isotopes measured during analysis vary between sessions (ESI 1†).[10] Isotopes measured in each session (with dwell times in milliseconds in parenthesis) are: ^{57}Fe (2), ^{185}Re (20), $^{185+14}$Re (50–80), ^{187}Os (20), $^{187+14}$Os (200), $^{188+14}$Os (10), $^{189+14}$Os (200).

The correction for reacted Re with the CH$_4$ gas was calculated using Os-free NIST612 glass using the mass shifted Re at masses 199 (^{185}Re^{12}CH$_2$) and 201 (^{187}Re^{12}CH$_2$) and the methodology presented in ref. 5 and 6 assuming natural Re abundances (^{185}Re/^{187}Re = 0.59738 ± 0.00039 (ref. 11)).[11] Subsequently, an in-house Moly Hill molybdenite was used to calibrate the Re/Os ratio of the Henderson and Bingham molybdenites assuming an age of 2680 ± 90 Ma (^{187}Os/^{187}Re = 0.04566 ± 0.00153).[12] Note that this is a different piece of Moly Hill molybdenite to the reference material characterised in ref. 6 ^{188}Os/^{187}Os ratios are not reported for the USGS data as all ^{189}Os data (used as a proxy for ^{188}Os) were effectively below detection limit. Data reduction, involving background subtraction, interference, drift corrections, and ratio normalisation, were conducted using the LADR software v. 1.1.7.[13] Given interference subtracted count rates on $^{187+14}$Os in the time-resolved signals fall occasionally below zero, LADR fails to accurately calculate the signal precision uncertainty on the corrected ^{185}Re/$^{187+14}$Os ratios. Hence, signal precision uncertainties were calculated manually using spreadsheets by setting negative values to zero prior to calculating the standard deviation on the $^{187+14}$Os signal. All other sources of uncertainty (Table 1) are subsequently propagated to the calculated signal precision uncertainties. Reported fully propagated uncertainties on the isotope ratios are 2 SEM. No correction for downhole Re–Os fractionation was made.[6] Age calculations were conducted as weighted means in IsoplotR from the corrected ^{187}Os/^{187}Re ratios[14] and age uncertainties are reported as 95% confidence uncertainties.

Adelaide microscopy

At Adelaide microscopy, Re–Os isotope analysis was conducted on a RESOlution-SE 193 nm laser ablation system coupled to an Agilent 8900× ICP-MS/MS over two analytical sessions. The molybdenites were sampled by static spot ablation at 3 J cm^{-2} and the aerosol was transported to the plasma in a gas atmosphere of 1 l min^{-1} Ar, 0.38 l min^{-1} He and 4 ml min^{-1} N$_2$. Given the absence of Re–Os down-hole fractionation,[6] laser beam diameters and repetition rates were variable (30–100 μm, 7–10 Hz) between reference materials and samples, with the aim to maximize count rates while keeping Re count rates under the pulse/analog threshold for the detector (see ESI 1† for details).

For each session, the mass-spectrometer was first tuned in absence of reaction gas to demonstrate a robust plasma (e.g. ThO/Th rate of <0.2% and U/Th <1.1). Subsequently, for session 1, a mixture of CH$_4$ (0.22 ml min^{-1}) + He (5 ml min^{-1}) + H$_2$ (6 ml min^{-1}) was used in the reaction cell, tuned to maximise count rates. H$_2$ was used to enhance sensitivity, while He was

This journal is © The Royal Society of Chemistry 2025

J. Anal. At. Spectrom., 2025, **40**, 1394–1402 | **1395**

Table 1 Propagated uncertainties in the analytical workflow. S = session. 187 + X refers to the mass-shift on Os with X being 14 amu for CH_4 and 64 amu for N_2O

Propagated uncertainties

Systematic uncertainties	Adelaide			USGS					
	S1: 7/12/2023	S2a: 14/12/2023	S2b: 14/12/2023	S1: 17/11/2021	S2: 22/11/2021	S3: 23/11/2021	S4: 4/07/2022	S5: 29/9/2023	S6: 26/6/2024
Calibration curve missfit Re/Os ratio	0.92%	0.86%	1.69%	1.39%	1.71%	0.61%	1.02%	0.74%	0.56%
Calibration curve missfit Os/Os ratio	0.55%	0.62%	0.62%	0.34%	0.38%	0.51%	0.72%	0.04%	0.24%
Uncertainty in measured Re/Os ratio for RM (Qmoly Hill)	0.11%	0.14%	0.24%	0.36%	0.25%	0.24%	0.50%	0.26%	0.24%
Uncertainty in measured Os/Os ratio for RM (NiS3)	0.09%	0.14%	0.14%	0.23%	0.21%	0.20%	0.32%	0.16%	0.11%
Uncertainty in mass bias	0.04%	0.12%	0.11%	0.34%	0.37%	0.35%	0.24%	0.34%	0.14%
Long-term reproducibility of reference materials	Not propagated uncertainties (insufficient data)								

Random uncertainties

Signal precision of interference corrected $^{187+X}$Os
Signal precision of ^{185}Re
Signal precision of $^{189+X}$Os
Uncertainty in blank subtraction
Uncertainty in interference correction factor (~signal precision of $^{185+X}$Re)
Added age uncertainty for overdispersion if present (IsoplotR)

Constants

Uncertainty in reference	0.38%
IDTIMS Re/Os ratio for RM (Qmoly Hill)	
Theoretical uncertainty in reference Os/Os ratio for RM (NiS3)	0.10%
Uncertainty in decay constant (IsoplotR default)	0.51%
Uncertainty in initial Os/Os ratio anchor (IsoplotR default)	0.06%

Table 2   Analytical results for reference materials and molybdenites from Bingham Canyon and Henderson[a]

Session	Reaction gas	n[c]	^{185}Re (cps)	±2SEM	$^{185-x}$Re (cps)	±2SEM	$^{187+x}$Os[b] (cps) Measured	±2SEM	$^{187+x}$Os[b] (cps) Corrected[d]	±2SEM	Interf.[e] (%)	[f]Re RR (%)	Age (Ma)[g]	±CI (Ma)	±CI[h] (%)	MSWD[i]
Adelaide																
QMolyHill primary RM (IDTIMS: 2624 ± 5 Ma)																
1	CH$_4$ + He + H$_2$	30	545 008	58 015	3120	334	30 097	3184	24 746	2611	18%	0.57%	2625	9|28	1.1%	1.0
2a	N$_2$O	16	462 690	97 879	863	198	24 508	5605	23 023	5265	6%	0.19%	2625	12|29	1.1%	1.0
2b	N$_2$O + He	6	518 434	95 257	118	19	14 167	2783	13 968	2750	2%	0.02%	2624	38|46	1.8%	1.0
M252 secondary RM (IDTIMS: 1520 ± 4 Ma)																
1	CH$_4$ + He + H$_2$	30	790 180	149 834	4463	838	27 946	5283	20 307	3848	28%	0.56%	1505	6.5|16	1.1%	0.83
2a	N$_2$O	16	1 574 831	243 405	2766	418	46 691	7116	41 929	6397	10%	0.18%	1500	11|20	1.3%	1.9
2b	N$_2$O + He	6	1 953 411	761 730	474	196	29 925	11 571	29 107	11 235	3%	0.02%	1514	23|28	1.8%	0.5
Bingham (IDTIMS: 37.0 ± 0.27 Ma)																
1	CH$_4$ + He + H$_2$	28	879 007	64 792	5150	379	9499	701	683	168	93%	0.59%	45.4	1.9|2.0	4.4%	0.62
2a	N$_2$O	18	724 950	33 786	1193	58	2495	121	443	68	83%	0.16%	36.5	1.3|1.3	3.6%	0.52
2b	N$_2$O + He	18	711 728	38 923	157	9	542	29	272	30	49%	0.02%	37.9	0.9|1.0	2.6%	0.35
Henderson (IDTIMS: 27.656 ± 0.022 Ma)																
1	CH$_4$ + He + H$_2$	26	200 280	27 584	1185	162	2151	296	121	38	95%	0.59%	30.9	3.9|3.9	13%	3.7
2a	N$_2$O	18	117 332	11 678	188	19	375	39	50	14	87%	0.16%	23.3	3.1|3.1	13%	3.3
2b	N$_2$O + He	18	96 570	8575	23	2	66	6	26	7	58%	0.02%	27.5	1.6|1.6	5.8%	1.6

Session	Reaction gas		^{185}Re (cps)	±2SEM	$^{185-x}$Re (cps)	±2SEM	$^{187+x}$Os[b] (cps) Measured	±2SEM	$^{187+x}$Os[b] (cps) Corrected[c]	±2SEM	Interf.[d] (%)	Re RR[e] (%)	Age[f] (Ma)	±CI[g] (Ma)	±CI[g] (%)	MSWD[h]
USGS																
Moly Hill primary RM (IDTIMS: 2680 ± 90 Ma)																
1	CH$_4$ + He + H$_2$	9	866 292	213 714	2719	669	36 328	9056	31 705	7916	13%	0.31%	2687	28|36	1.3%	11
2	CH$_4$ + He + H$_2$	11	2 046 608	357 149	6674	1141	93 533	16 383	82 195	14 448	12%	0.33%	2689	28|38	1.4%	0.7
3	CH$_4$ + He + H$_2$	10	1 332 768	251 245	4248	803	60 408	11 493	53 172	10 124	16%	0.32%	2687	12|29	1.1%	1.6
4	CH$_4$ + He + H$_2$	12	1 167 149	191 059	12 850	2580	65 312	12 677	43 514	8495	33%	1.10%	2689	24|36	1.3%	0.7
5	CH$_4$ + He + H$_2$	14	644 773	127 330	2605	521	42 428	8206	38 015	7334	10%	0.40%	2690	12|29	1.1%	0.7
6	CH$_4$ + He + H$_2$	19	466 349	62 345	1927	255	30 604	3972	27 306	3539	10%	0.41%	2690	2.7|27	1.0%	0.8
Bingham (IDTIMS: 37.0 ± 0.27 Ma)																
1	CH$_4$ + He + H$_2$	5	1 063 763	241 044	3379	778	6256	1425	500	152	92%	0.32%	36.1	4.8|4.8	13%	0.6
2	CH$_4$ + He + H$_2$	6	1 359 430	106 220	4678	359	8729	658	772	201	91%	0.34%	39.5	4.1|4.1	10%	0.9
3	CH$_4$ + He + H$_2$	5	2 449 963	461 924	7805	1456	14 820	2771	1545	333	90%	0.32%	42.9	4.1|4.1	9.6%	0.04
4	CH$_4$ + He + H$_2$	8	1 756 781	283 965	18 551	3035	32 826	5334	1352	423	96%	1.06%	36.9	4.0|4.0	11%	0.9
5	CH$_4$ + He + H$_2$	10	880 153	88 079	3518	358	7010	629	777	265	86%	0.40%	40.0	3.5|3.5	8.8%	0.5
6	CH$_4$ + He + H$_2$	16	450 317	48 575	1809	198	3459	384	372	175	88%	0.40%	33.2	5.2|5.2	16%	2.6

This journal is © The Royal Society of Chemistry 2025

J. Anal. At. Spectrom., 2025, 40, 1394–1402 | 1397

JAAS
Paper

Table 2 (Contd.)

Session	Reaction gas	n	^{185}Re (cps)	±2SEM	$^{185+x}$Re (cps)	±2SEM	$^{187+x}$Os^b (cps) Measured	±2SEM	$^{187+x}$Os^b (cps) Corrected^c	±2SEM	Interf.^{d} (%)	Re RR^e (%)	Age^f (Ma)	±CI^g (Ma)	±CI^g (%)	MSWD^h
USGS																
Henderson (IDTIMS: 27.656 ± 0.022 Ma)																
1	CH$_4$ + He + H$_2$	8	292 726	15 817	930	44	1701	95	116	37	93%	0.32%	25.5	5.9|5.9	23%	2.8
2	CH$_4$ + He + H$_2$	6	126 604	26 237	434	91	794	164	59	20	93%	0.34%	29.4	9.1|9.1	31%	4.6
3	CH$_4$ + He + H$_2$	8	463 603	10 291	1497	34	2759	58	216	56	93%	0.32%	29.3	4.5|4.5	15%	2.8
4	CH$_4$ + He + H$_2$	14	453 338	11 020	4537	115	8002	196	288	109	96%	1.00%	22.1	6.7|6.7	30%	6.9
5	CH$_4$ + He + H$_2$	11	93 184	15 293	380	62	714	120	60	22	91%	0.41%	20.1	5.6|5.6	28%	5.4
6	CH$_4$ + He + H$_2$	17	161 548	34 540	644	135	1205	253	93	40	90%	0.40%	26.1	3.3|3.3	13%	1.7

^{a} All cps (=counts per second) values are back-ground subtracted. ^{b} $x = 14$ amu for CH$_4$ reaction to OsCH$_2^+$, $= 64$ amu for N$_2$O reaction to OsO$_4^+$. ^{c} n = Number of analyses per sample. ^{d} Corrected refers to the interference correction of $^{187+x}$Re on $^{187+x}$Os by cps subtraction. ^{e} Interf. is the percentage interference of $^{187+x}$Re on $^{187+x}$Os. ^{f} Re RR is the Re reaction rate calculated as the ratio of $^{185+x}$Re on ^{185}Re. ^{g} Age is the calculated weighted mean Re–Os age in IsoplotR. ^{h} ±CI is the 95% confidence interval uncertainty on the age, calculated using added uncertainty for over dispersion where required. The second number also includes the uncertainty on the decay constant. % is only reported for the maximum propagated uncertainty. ^{i} MSWD = Mean squared weighted deviation.

used to buffer ^{187}Re^{12}CH$_2$ interference production. In the second session, N$_2$O (0.32 ml min^{-1}) was used as the reaction gas, first (session 2a) without added He (maximum sensitivity) and secondly (session 2b) with added He (5 ml min^{-1}) to reduce the interference. Lense parameters and reaction cell settings were similar between both methods, detailed in ESI 1.† The isotopes measured during analysis vary between sessions (ESI 1†). Isotopes measured in each session (with dwell times in milliseconds in parenthesis) are: ^{95}Mo (2), ^{185}Re (20), $^{185+X}$Re (50–100), ^{187}Os (50), $^{187+X}$Os (100), ^{189}Os (50), $^{189+X}$Os (100–200). $^{189+X}$Os was measured as a proxy for 'common' ^{188}Os.

The measured ^{185}Re/$^{187+x}$Os ratios (with $x = 14$ amu for CH$_4$ method, $x = 64$ amu for N$_2$O method) were corrected for $^{187+x}$Re interference on $^{187+x}$Os, taking into account the mass-bias on the ^{187}Re/^{185}Re ratio, measured in Os-free NIST610 glass (see details in ESI 1†), and subsequently calibrated to the QMolyHill reference molybdenite (N-TIMS ^{187}Os/^{187}Re ratio = 0.044699 ± 0.000166, age = 2624 ± 5 Ma, 2SEM uncertainties[6]). The ^{188}Os/^{187}Os ratios were calibrated using NiS-3,[15] using measured $^{189+X}$Os as a proxy for ^{188}Os and assuming a present-day ^{188}Os/^{187}Os ratio of 6.740 ± 0.004.[16] Data reduction, involving background subtraction, interference, drift corrections, and ratio normalisation, were conducted using the LADR software v. 1.1.7.[13] As above, signal precision uncertainties were calculated manually using a script by setting negative values to zero prior to calculating the standard deviation on the $^{187+14}$Os signal. All other sources of uncertainty (Table 1) are subsequently propagated to the calculated signal precision uncertainties. Reported fully propagated uncertainties on the isotope ratios are 2 SEM. Age calculations were conducted as weighted means in IsoplotR from the corrected ^{187}Os/^{187}Re ratios[14] and age uncertainties are reported as 95% confidence uncertainties.

Reference molybdenite M252 from the Merlin deposit (Queensland, Australia) was used as secondary reference material to verify accuracy in isotope ratio determinations (N-TIMS ^{187}Os/^{187}Re ratio = 0.025649 ± 0.000105, age = 1520 ± 4 Ma (ref. 6)). The obtained Re–Os dates are 1505 ± 16 Ma (session 1), 1500 ± 20 Ma (session 2a) and 1514 ± 28 Ma (session 2b), in agreement with the reference age. Isotopic ratio uncertainties and age uncertainties are quoted as 2 standard error of the mean.

Results

Sensitivity and interferences

For the USGS sessions (all with CH$_4$ + H$_2$ + He reaction gas, abbreviated as U-sessions), the average sensitivity measured for a 40 µm/10 Hz laser beam on ^{185}Re (measured on NIST-612) varied between *ca.* 5.7 and 10.3 kcps ppm^{-1}. For the Adelaide sessions (with variable reaction gas mixtures, abbreviated as A-sessions), the average sensitivity for a 50 µm/10 Hz spot ablation on ^{185}Re (measured on NIST-610) was 9.1 kcps ppm^{-1} for A-session 1 (CH$_4$ + H$_2$ + He), 7.3 kcps ppm^{-1} for A-session 2a (N$_2$O), and 6.3 kcps ppm^{-1} for A-session 2b (N$_2$O + He). While the CH$_4$-method (U-sessions and A-session 1) produced the highest sensitivity, it also induced the highest Re interference with *ca.* 0.5% (average USGS) and *ca.* 0.6% (average Adelaide) Re
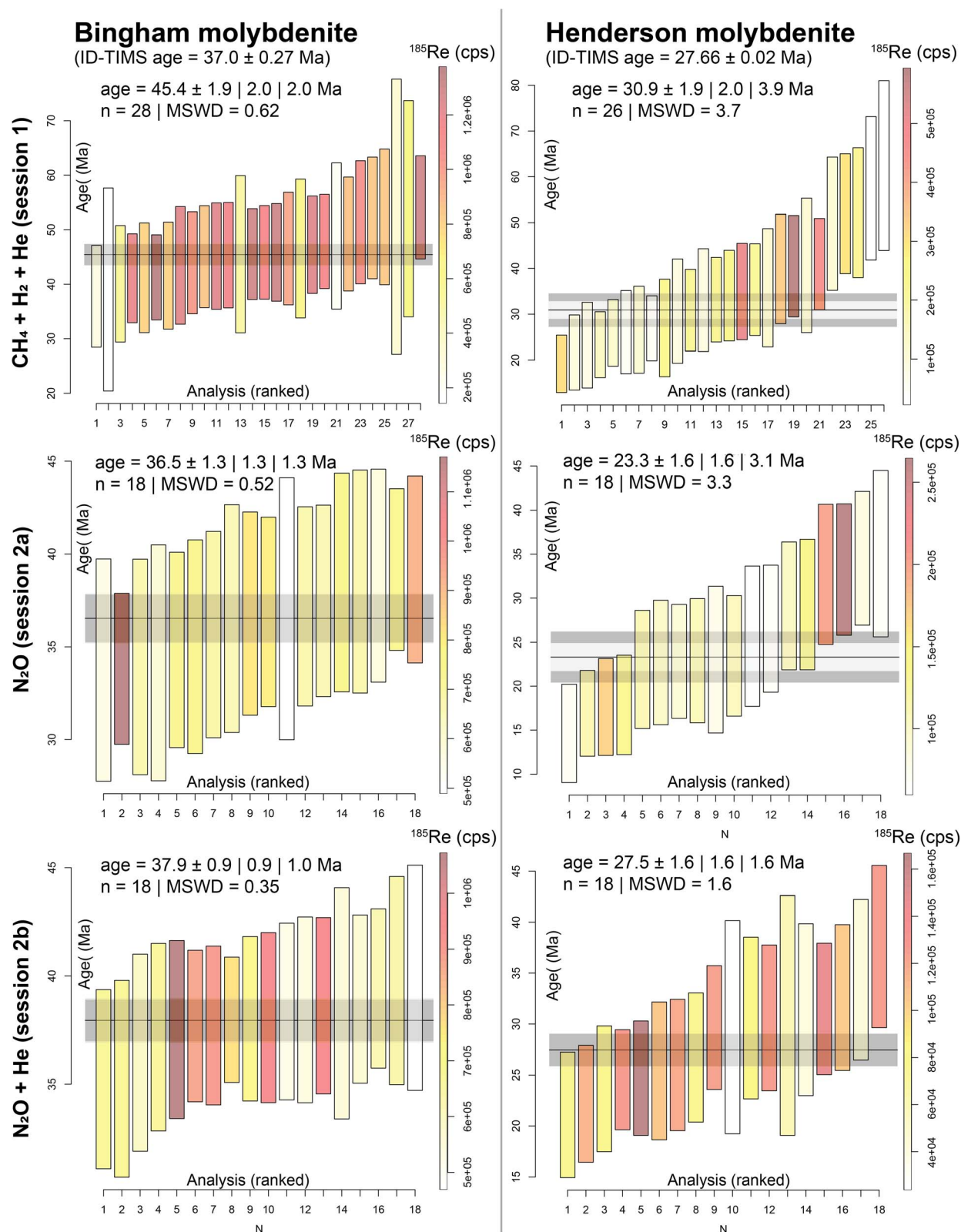
Fig. 1 *In situ* Re–Os dates for the Bingham and Henderson molybdenite, analysed at Adelaide Microscopy, calculated as weighted means in IsoplotR.[14] Analyses are ranked by age, plotted with 2 SEM uncertainties, and colour coded to ^{185}Re count rate (cps). Reported weighted mean age uncertainties are 95% confidence intervals, without overdispersion, with overdispersion and with added uncertainty on the decay constant. MSWD = mean squared weighted deviation on the weighted mean Re–Os date.

This journal is © The Royal Society of Chemistry 2025

J. Anal. At. Spectrom., 2025, **40**, 1394–1402 | **1399**

reacting to form $ReCH_2^+$ (Table 2). This is *ca.* 45–65% lower compared to previously reported Re reaction rates in absence of H_2 in the reaction cell.[6,7] For the N_2O method, *ca.* 0.17% Re reacts to the equivalent ReO_4^+ reaction product (A-session 2a), which is further reduced to 0.02% with added He (5 ml min-1; A-session 2b). Hence, although count rates are compromised, the N_2O + He method requires a much smaller $^{187+x}$Re interference correction on $^{187+x}$Os. For example, on the secondary reference molybdenite (M252), the interference correction requires removal of 28% Re from Os on mass 187 + 14 amu in A-session 1, 10% on mass 187 + 64 amu for A-session 2a and 3% on mass 187 + 64 amu for A-session 2b (Table 2). Applied to the Cenozoic molybdenite samples, which are much younger and thus have considerably less radiogenic ^{187}Os ingrowth compared to the Mesoproterozoic M252 molybdenite, the interference correction

accounts for *ca.* 87–97% in the U-Sessions, 93–95% in A-session 1, 83–87% in A-session 2a and 49–58% in A-session 2b.

Cenozoic molybdenite Re–Os dates

The extensive interference subtraction significantly affects the accuracy and precision (as a function of count rate statistics and age dispersion) of the *in situ* Re–Os dates (Table 2 and Fig. 1). When CH_4 + H_2 + He is used in the reaction cell (A-session 1, all U-sessions), the Re–Os dates for the Henderson molybdenites are consistently over-dispersed (MSWD between 1.7 and 6.9) and at least for one analytical session (U5), the resulting weighted mean Re–Os date is too young (20.1 ± 5.6 Ma) compared to the IDTIMS reference age (27.66 ± 0.02 Ma; Fig. 1, 2 and Table 2). For the Bingham molybdenites, the CH_4 + H_2 + He method in Adelaide (A-session 1) produced an inaccurate
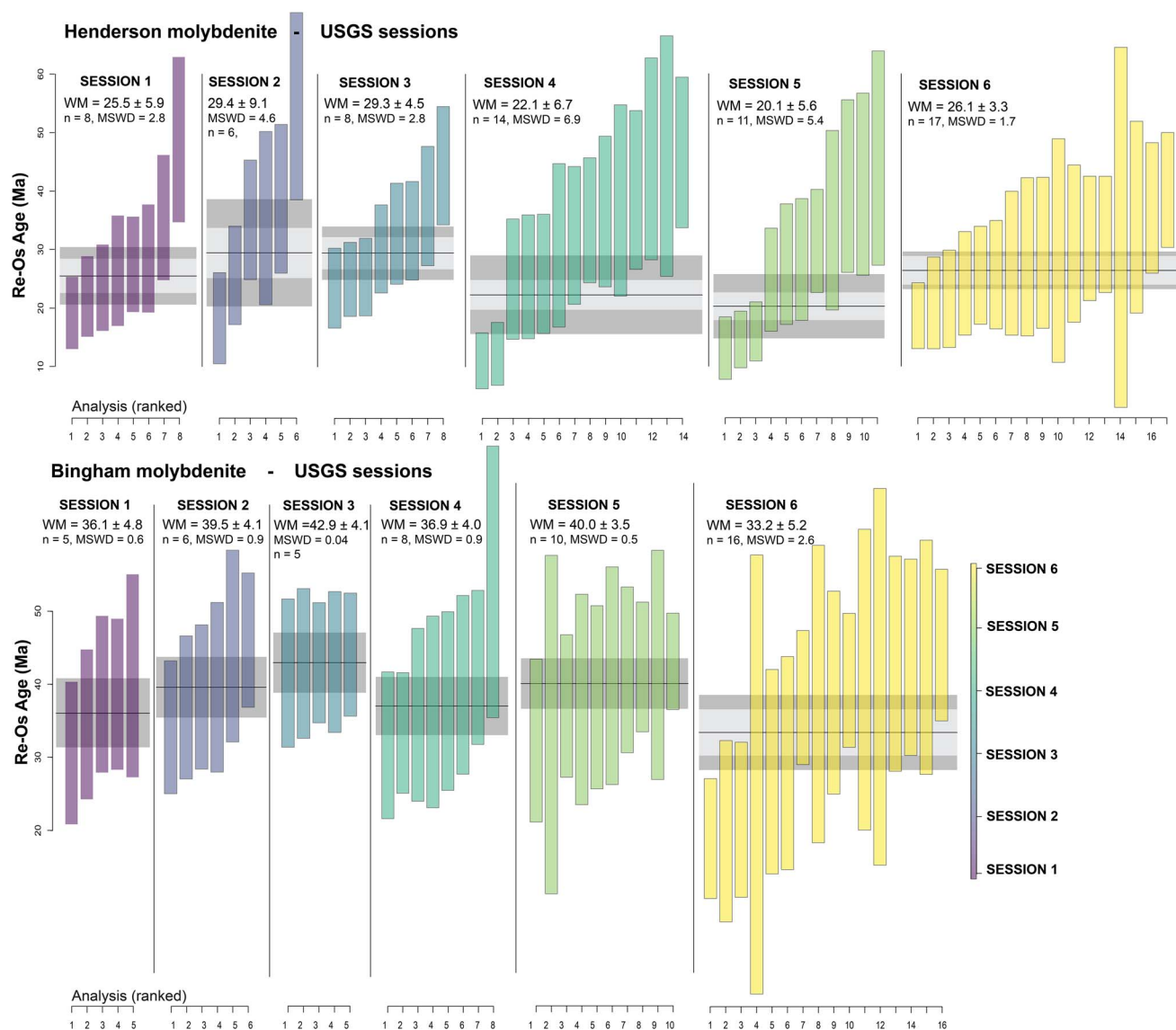

Fig. 2 *In situ* Re–Os dates for the Bingham and Henderson molybdenite, analysed at the U.S. Geological Survey (USGS), calculated as weighted means in IsoplotR.[14] Analyses are ranked by age and plotted with 2 SEM uncertainties. The resulting Re–Os age uncertainties are 95% confidence intervals including overdispersion (other uncertainties are shown in Tables 1 and 2). MSWD = mean squared weighted deviation on the weighted mean Re–Os date.

1400 | *J. Anal. At. Spectrom.*, 2025, **40**, 1394–1402

This journal is © The Royal Society of Chemistry 2025

date of 45.4 ± 2.0 Ma, compared to the IDTIMS reference age of 37.0 ± 0.3 Ma (Fig. 1 and Table 2). Furthermore, precision is compromised with the $CH_4 + H_2 + He$ method, producing fully propagated age uncertainties up to 13% in Adelaide and as high as 31% at the USGS. Age precision and accuracy is improved with the N_2O reaction gas (A-session 2a), producing dates of 36.5 ± 1.3 Ma for Bingham (in agreement with reference age) and 23.3 ± 3.1 Ma for Henderson (younger than reference age). Age dispersion remains large for Henderson with an MSWD of 3.3. For A-session 2b, where He is added to N_2O in the reaction cell, both molybdenite dates are accurate and at the highest precision: 37.9 ± 1.0 Ma (2.6% uncertainty) for Bingham and 27.5 ± 1.6 Ma (5.8% uncertainty) for Henderson. For both samples, the dataset statistically constitutes a single age population (MSWD = 0.35 for Bingham and 1.6 for Henderson). For the $N_2O \pm He$ sessions, the background and interference subtracted count rates on $^{187+64}Os$ are ≤ 50 cps for the Henderson molybdenite, approaching the limits of the analytical method, while still producing accurate and precise dates.

Discussion

Interference correction in function of reaction rate and age

While it's important to maximize sensitivity (total count rates), the magnitude of the interference correction of $^{187+x}Re$ on $^{187+x}Os$ exerts a dominant control on the accuracy of *in situ* Re–

Fig. 3 Percentage $^{187+x}Re$ interference on $^{187+x}Os$ plotted as a function of age for the three Adelaide analytical sessions with different reaction gas mixtures. Open symbols represent measured interference percentages (M.), while filled symbols were theorized (T.) based on a theorical formula from ref. 7. The curves are second-order interpolation polynomials (I.) for the theorized values. RR refers to the Re reaction rate (ratio of $^{185+x}Re/^{185}Re$), λ is the decay constant, t is age in Ma and F is a method-specific ^{187}Os transmission factor. For the CH_4 and N_2O methods, F was adapted from ref. 7 For the new $N_2O + He$ method, F was calculated as the ratio between measured and predicted interference curves. This plot can be used to predict the interference percentage based on age and method-specific constants (RR and F).

Os age results, especially for young samples. Hence, an ability to predict the percentage interference would be an important screening tool prior to Re–Os analysis, increasing the likelihood of useful age calculations. Simpson *et al.*[7] determined the interference as a function of Re reaction rate and age: $^{187+x}Re$ (%) = RR $\times [F \times (e^{\lambda t} - 1) + RR]^{-1}$. Given RR (= Re reaction rate) and F (=^{187}Os transmission factor) are reaction-gas specific constants that should be largely invariable once determined for given mass-spectrometer tuning conditions, the interference correction can be predicted in function of age (Fig. 3). For Palaeogene (*ca.* 66–23 Ma) molybdenite, the interference is predicted to vary between *ca.* 87% and 95% for the $CH_4 + H_2 + He$ reaction gas and between *ca.* 72% and 88% for the N_2O reaction gas. Unless very high count rates can be measured (Re-rich molybdenite), such large correction will lead to over-dispersed and likely inaccurate dates, assuming that the samples are internally homogenous in terms of Re–Os ratios. For the $N_2O + He$ method, the interference correction remains significant (*ca.* 35–60%) but we demonstrate accurate and robust dates can be obtained with this approach.

Limitations and advantages of *in situ* Re–Os geochronology

Compared to the conventional ID-TIMS approach, higher sensitivity is required to enable accurate age determination by LA-ICP-MS/MS for young molybdenites. Therefore, Re concentrations need to be sufficiently high (^{185}Re >100k cps) before attempting *in situ* Re–Os analysis. As demonstrated, an optimized gas mixture is crucial to minimize interference from $^{187+x}Re$ on $^{187+x}Os$, with the $N_2O + He$ reaction gas being most promising. However, for older (Precambrian) molybdenites, Simpson *et al.*[7] demonstrated fewer differences in obtainable age precision comparing reaction gasses, with the CH_4 method potentially giving better precision for >1 Ga molybdenites. Thus, different reaction gas mixtures should be evaluated as some cater better for old *versus* young molybdenite samples.

In contrast to ID-TIMS, which relies on bulk sample dissolution methods, the *in situ* method is a micro-sampling technique that has the ability to evaluate potential age zonation and/or isotopic disturbance (heterogeneity) across crystals. While age heterogeneity was not observed in the samples for this study (within the obtainable precision of a single analysis), the *in situ* technique is suitable for homogeneity assessments. Isotopic decoupling has been described previously[3,17] but was not observed within the resolution of our analyses.

However, the most important advantage of the *in situ* method is the speed of analysis, where up to 1000 single spot dates can be obtained within a single (*ca.* 24 hours) analytical session. This opens a new window of opportunities for mineral exploration (*e.g.* ref. 18) that can now be extended to young (Palaeogene) molybdenite systems when Re concentrations are sufficiently high.

Conclusions

We evaluated three reaction gas mixtures for *in situ* (LA-ICP-MS/MS) Re–Os geochronology of young (Cenozoic) molybdenites
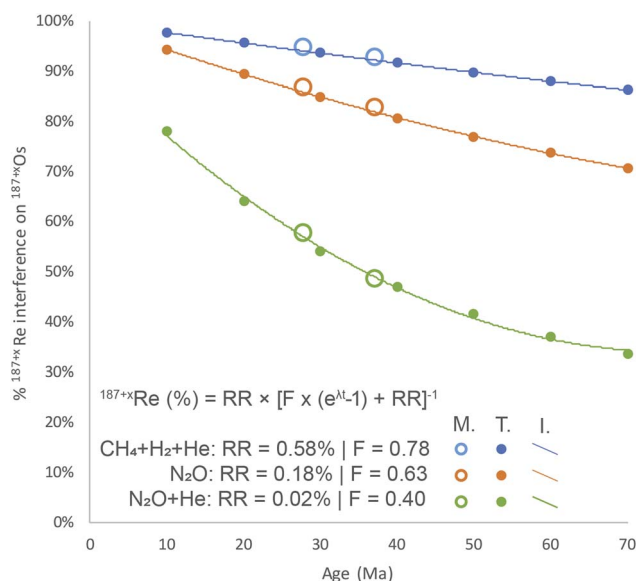
This journal is © The Royal Society of Chemistry 2025

J. Anal. At. Spectrom., 2025, **40**, 1394–1402 | **1401**

and demonstrate that N_2O (0.3 ml min^{-1}) + He (5 ml min^{-1}) is the optimal reaction gas mixture to sufficiently reduce the isobaric interference of Re onto Os (*ca.* 0.02% Re reaction rate). Robust Re–Os dates were obtained for the Re-rich Palaeogene Bingham Canyon and Henderson molybdenite, validating the approach.

Data availability

All isotope ratio data and meta-data (reference materials, instrument conditions) are provided in the ESI† and ref. 10.

Author contributions

Conflicts of interest

There are no conflicts to declare.

Acknowledgements

References

1 N. J. Saintilan, D. Selby, R. A. Creaser and S. Dewaele, *Sci. Rep.*, 2018, **8**, 14946.

2 A. J. Finlay, D. Selby and M. J. Osborne, *Geology*, 2011, **39**, 475–478.

3 D. Selby and R. A. Creaser, *Geochim. Cosmochim. Acta*, 2004, **68**, 3897–3908.

4 H. J. Stein, R. J. Markey, J. W. Morgan, J. L. Hannah and A. Scherstén, *Terra Nova*, 2001, **13**, 479–486.

5 K. J. Hogmalm, I. Dahlgren, I. Fridolfsson and T. Zack, *Miner. Deposita*, 2019, **54**, 821–828.

6 R. Tamblyn, S. Gilbert, S. Glorie, C. Spandler, A. Simpson, M. Hand, D. Hasterok, B. Ware and S. Tessalina, *Geostand. Geoanal. Res.*, 2024, **48**, 393–410.

7 A. Simpson, S. Glorie, S. Gilbert, R. Tamblyn and M. G. Gadd, *Chem. Geol.*, 2024, **670**, 122384.

8 J. T. Chesley and J. Ruiz, in *Geology and Ore Deposits of the Oquirrh and Wasatch Mountains*, Society of Economic Geologists, Utah, 1998, vol. 29.

9 R. Markey, H. J. Stein, J. L. Hannah, A. Zimmerman, D. Selby and R. A. Creaser, *Chem. Geol.*, 2007, **244**, 74–87.

10 J. M. Thompson and A. K. Souders, Re-Os Geochronology of Molybdenite and Metalliferous Black Shales, *U.S. Geological Survey Data Release*, 2025, DOI: **10.5066/P13ZTY3I.**

11 J. W. Gramlich, T. J. Murphy, E. L. Garner and W. R. Shields, *J. Res. Natl. Bur. Stand., Sect. A*, 1973, **77**, 691–698.

12 K. Suzuki, L. Qi, H. Shimizu and A. Masuda, *Geochim. Cosmochim. Acta*, 1993, **57**, 1625–1628.

13 A. Norris and L. Danyushevsky, *Towards estimating the complete uncertainty budget of quantified results measured by LA-ICP-MS*, Goldschmidt, Boston, 2018.

14 P. Vermeesch, *Geosci. Front.*, 2018, **9**, 1479–1493.

15 S. Gilbert, L. Danyushevsky, P. Robinson, C. Wohlgemuth-Ueberwasser, N. Pearson, D. Savard, M. Norman and J. Hanley, *Geostand. Geoanal. Res.*, 2013, **37**, 51–64.

16 J. Völkening, T. Walczyk and K. G. Heumann, *Int. J. Mass Spectrom. Ion Processes*, 1991, **105**, 147–159.

17 H. Stein, A. Scherstén, J. Hannah and R. Markey, *Geochim. Cosmochim. Acta*, 2003, **67**, 3673–3686.

18 A. Simpson, S. Glorie, M. Hand, S. E. Gilbert, C. Spandler, M. Dmitrijeva, G. Swain, A. Nixon, J. Mulder and C. Münker, *Geosci. Front.*, 2024, **15**, 101867.

1402 | *J. Anal. At. Spectrom.*, 2025, **40**, 1394–1402

This journal is © The Royal Society of Chemistry 2025